



MARS: A protein family involved in the formation of vertical skeletal elements



Shai Abehsera^{a,b}, Shani Peles^a, Jenny Tynyakov^c, Shmuel Bentov^b, Eliahu D. Aflalo^{a,b}, Shihao Li^d, Fuhua Li^d, Jianhai Xiang^d, Amir Sagi^{a,b,*}

^a Department of Life Sciences, Ben-Gurion University of the Negev, Beer-Sheva, Israel

^b National Institute for Biotechnology in the Negev, Ben-Gurion University of the Negev, Beer-Sheva, Israel

^c Steinitz Marine Biology Laboratory, Interuniversity Institute for Marine Sciences, Department of Zoology, Tel Aviv University, Tel Aviv, Israel

^d Key Laboratory of Experimental Marine Biology, Institute of Oceanology, Chinese Academy of Sciences, Qingdao, China

ARTICLE INFO

Article history:

Received 12 February 2017

Received in revised form 4 April 2017

Accepted 5 April 2017

Available online 7 April 2017

Keywords:

Crustacean mandible

Chitin fibers

MARS proteins

Structural proteins

Tooth structure

Vertical elements

ABSTRACT

Vertical organizations of skeletal elements are found in various vertebrate teeth and invertebrate exoskeletons. The molecular mechanism behind the development of such structural organizations is poorly known, although it is generally held that organic matrix proteins play an essential role. While most crustacean cuticular organizations exhibit horizontal chitinous layering, a typical vertical organization is found towards the surface of the teeth in the mandibles of the crayfish *Cherax quadricarinatus*. Candidate genes encoding for mandible-forming structural proteins were mined in *C. quadricarinatus* molt-related transcriptomic libraries by using a binary patterning approach. A new protein family, termed the Mandible Alanine Rich Structural (MARS) protein family, with a modular sequence design predicted to form fibers, was found. Investigations of spatial and temporal expression of the different MARS genes suggested specific expression in the mandibular teeth-forming epithelium, particularly during the formation of the chitinous vertical organization. MARS loss-of-function RNAi experiments resulted in the collapse of the organization of the chitin fibers oriented vertically to the surface of the crayfish mandibular incisor tooth. A general search of transcriptomic libraries suggested conservation of MARS proteins across a wide array of crustaceans. Our results provide a first look into the molecular mechanism used to build the complex crustacean mandible and into the specialized vertical structural solution that has evolved in skeletal elements.

© 2017 Elsevier Inc. All rights reserved.

1. Introduction

In the animal kingdom, skeletal elements characterized by a vertical or perpendicular orientation relative to the surface of the element are to be found in some high-impact and/or load-bearing regions of the skeleton (Al-Sawalmih et al., 2008). An excellent example of such vertical elements is the vertebrate tooth in which the outer enamel layer consists of apatite rods oriented vertically to the tooth surface (Lucas, 2004). Examples in terrestrial and aquatic invertebrates include the mollusk shell, in which an outer prismatic layer mineralized with calcite rods is oriented vertically to the surface (Chateigner et al., 2000; DiMasi and Sarikaya, 2004), and the crustacean cuticle, in which an outer mineralized layer containing calcite crystals is vertically oriented on a scaffold

of vertically oriented chitin fibers (Al-Sawalmih et al., 2008). Two particularly representative examples in the invertebrates are the vertical arrangement of non-mineralized fibers in the incisor tooth tip of the terrestrial crustacean isopod *Porcellio scaber* (Huber et al., 2014) and the enamel-like apatite structure oriented vertically to the surface of the molar tooth in the mandibles of our study species, the crayfish *Cherax quadricarinatus* (Bentov et al., 2012). This vertical orientation structural solution that is prevalent in the animal kingdom suggests convergent evolution in different invertebrates and vertebrates. However, although the structural aspects have been well researched, the molecular and biochemical mechanisms underlying the formation of such vertical elements remain to be revealed.

In *C. quadricarinatus*, the two mandibles form the anterior mouthparts, located directly in front of the oral opening. Each mandible consists of a large basal segment that is capped with two teeth, the molar tooth, serving as a massive grinding surface for mastication, and the incisor, whose function is grabbing and

* Corresponding author at: Department of Life Sciences, Ben-Gurion University of the Negev, Beer-Sheva, Israel.

E-mail address: sagia@bgu.ac.il (A. Sagi).

holding food. Similarly to other cuticular structures, the mandibles and teeth of crustaceans are replaced during each molt cycle (Bentov et al., 2012). The crustacean molt cycle comprises four stages: inter-molt, pre-molt, ecdysis and post-molt. Following the inter-molt stage between two molting events, pre-molt comprises partial resorption of the old exoskeleton in parallel to the initial formation of the new exoskeleton. The outer non-chitinous epicuticle and the middle chitinous layer the exocuticle are formed during this stage. Following pre-molt, ecdysis – the actual shedding the old exoskeleton – takes place. In the post molt stage, the cuticle fully forms and hardens by mineralization (Roer and Dillaman, 1984). Unlike most the rest of the exoskeleton of the crayfish, the molar tooth is special in that it is already partially mineralized in the pre-molt stage (Tynyakov et al., 2015a). This type of pre-molt mineralization is known to exist in different tooth of other crustaceans, with the deposition of silica minerals in the mandibular tooth of calanoid copepods (Miller et al., 1990) and the ossicles of the gastric mill of the blue crab (Nesbit and Roer, 2016).

The formation and mineralization of extracellular matrixes, such as the mandibles of *C. quadricarinatus*, are controlled by an organic matrix. Important components of this organic matrix are structural proteins, which play a variety of roles in matrix formation (Weiner and Dove, 2003). In crustaceans, the expression of structural-protein genes is tightly linked to the progress of molt cycle events (Roer et al., 2015). This linkage may be exploited for the development of specialized study tools, one of which is the binary patterning approach developed in our laboratory. This tool was designed to assist the mining of molt-related proteins by clustering genes sharing a common pattern of expression during the molt cycle (Abehsera et al., 2015).

Assisted by the above binary patterning tool, we discovered a novel protein family, designated the Mandible Alanine Rich Structural (MARS) protein family. Here, we show that the MARS proteins are involved in the formation of the chitinous vertical skeletal organization towards the surface of the mandible incisor. Their putative role is reinforcement of these vertical elements in the direction of the normal axis, since their loss of function resulted in almost complete collapse of the vertical structure.

2. Materials and methods

2.1. Animals and molt induction

C. quadricarinatus crayfish were grown in and collected from artificial ponds at Ben-Gurion University of the Negev, Beer-Sheva, Israel. Food comprising shrimp pellets (Rangen Inc., Buhl, ID, USA, 30% protein) were supplied *ad libitum* three times a week. Temperature was kept at 27 ± 2 °C, and a photoperiod of 14 h light and 10 h dark was applied. Water quality was assured by circulating the entire volume of water through a bio-filter. The pH of the water was 8.3 ± 0.5 , the nitrite concentration was less than 0.1 mg/l, the nitrate concentration was less than 50 mg/l, ammonium levels were negligible, and oxygen levels exceeded 5 mg/l. For all molt induction experiments, inter-molt crayfish were held in individual cages and endocrinologically induced to enter pre-molt through daily α -ecdysone injections, as previously described (Abehsera et al., 2015). Progression of the molt cycle was monitored daily by measuring the gastrolith molt mineralization index (MMI), which is known to correlate with molt stages and hormonal titers (Shechter et al., 2008a). MMI values for the molt stages were: inter-molt, 0; early pre-molt, 0.02–0.04; and late pre-molt 0.1–0.2. Post-molt animals were harvested on the day following ecdysis. For all dissection procedures, crayfish were placed on ice for 10–15 min until they became anesthetized.

2.2. In-silico mining for candidate mandible-forming proteins

Mining for candidate mandible-forming proteins was conducted on the basis of our molt-related transcriptomic library (Abehsera et al., 2015). In brief, a reference *C. quadricarinatus* transcriptome was constructed from next generation sequencing (NGS) of samples originating from two types of forming epithelium—the molar tooth and the gastrolith. Animals in the four different molt stages were sampled for each type of forming epithelium: inter-molt (one pool of three animals, i.e., $n = 1$), early pre-molt (one pool of three animals, i.e., $n = 1$), late pre-molt (two single animals and one pool of two animals, i.e., $n = 3$) and post-molt (two single animals, i.e., $n = 2$). Filtering for candidate mandible-forming proteins was performed using the binary-patterning mining approach described earlier (Abehsera et al., 2015). With this approach, transcripts having a binary pattern concomitant with molar formation, hence high expression during pre-molt (binary pattern 0110), were grouped and viewed as potential candidates, thereby producing a list of candidate transcripts. This list was then submitted to several additional *in silico* mining filters. The first filter aimed at mining for candidates expressed uniquely in the molar-forming epithelium and not in the gastrolith-forming epithelium. The filtered candidate transcripts were then computationally translated to a protein using the translate tool from the ExpASY Proteomics Server (Gasteiger et al., 2005) (<http://ca.expasy.org/tools/dna.html>), and the longest open reading frame was selected as the putative protein sequence. Finally, as the last filter, we mined for candidate proteins possessing known structural protein features using the three following determinants: the presence of a signal peptide, which was calculated using SignalP 4.0 (Petersen et al., 2011), the abundance of repeating motifs, which was calculated using REPRO (George and Heringa, 2000), and the presence of predicted intrinsically unstructured regions, which was calculated using IUPRED (Dosztanyi et al., 2005). In addition, the mined candidate proteins were examined against the molt-related transcriptomic library with the aim to find possible paralogues using TBLASTX (Altschul et al., 1990).

2.3. Characterization of the MARS protein family

The complete mRNA sequence was confirmed using 3' and 5' rapid amplification of cDNA ends (CLONTECH Laboratories), performed according to the manufacturer's guidelines. Predicted protein sequences were analyzed using various bioinformatics tools. First, the amino acid content and predicted pI of each protein were calculated using the ProtParam tool from the ExpASY Proteomics Server (Gasteiger et al., 2005) (<http://web.expasy.org/protparam/>). Thereafter, to find sequence similarities, a Multiple Sequence Alignment (MSA) was constructed using Clustal Omega (Sievers and Higgins, 2014). The prediction of proprotein convertase cleavage sites using ProP 1.0 (Duckert et al., 2004) was conducted. The presence of intrinsically disordered regions and α -helices in the active protein was predicted using XtalPred web server (Slabinski et al., 2007).

2.4. Spatial-temporal expression

Spatial-temporal expression patterns of genes were examined using RT-PCR. Total RNA was isolated from the molar-forming epithelium, incisor-forming epithelium, carapace cuticle-forming epithelium, gastrolith-forming epithelium, hepatopancreas and abdominal muscle from males in four main molt stages (inter-molt, early pre-molt, late pre-molt and post-molt) using EZ-RNA Total RNA Isolation Kit (Biological Industries, Beit Haemek, Israel), according to the manufacturer's protocol. First-strand cDNA was synthesized by reverse transcription using the qScript cDNA Kit

(Quanta BioSciences, Gaithersburg, MD) with 1 µg of total RNA. Specific primers were used for PCR amplification, PCR was performed with REDTaq ReadyMix PCR Reaction Mix (Sigma); using specific conditions: 94 °C for 1 min, followed by 35 cycles of 94 °C for 1 min, 60 °C for 30 s, 72 °C for 1 min, followed by 10 min at 72 °C. *C. quadricarinatus 18S* (accession no. AF235966) amplification served as the RNA positive control.

2.5. In-vitro expression-pattern validation using qPCR

C. quadricarinatus males were induced for molting and then dissected in the different main molt stages (inter-molt, early pre-molt, late pre-molt and post-molt), as described above (n = 5 for each molt stage). RNA was extracted from the molar- and the incisor-forming epithelia, as described above. In addition, RNA was extracted from the muscle tissue of an inter-molt animal for normalization. First-strand cDNA was synthesized by means of a reverse transcriptase reaction, as described above. Relative quantification of transcript levels was performed using Roche Diagnostics FastStart Universal Probe Master Mix (Basel, Switzerland) and Roche Universal Probe Library probes. The following primers and probes were used: for *MARS1*, qMARS1 F and qMARS1 R, Probe #25; for *MARS2*, qMARS2 F and qMARS2 R, Probe #22; for *MARS3*, qMARS3 F and qMARS3 R, Probe #22; for *MARS4*, qMARS4 F and qMARS4 R, Probe #22. *C. quadricarinatus 18S*, which served as a normalizing gene, was also quantified by means of real-time RT PCR using the primers, qcq18S F and qcq18S R, Probe #22. All primer sequences are shown in Table S5. Reactions were performed with the ABI Prism7300 Sequence Detection System, Applied Biosystems (Foster City, CA). Statistical analyses for relative transcript levels between the molt stages were performed using the non-parametric Kruskal-Wallis rank sum test, followed by multiple pair-wise comparisons using the Wilcoxon rank sum test; $p < 0.05$ was considered statistically significant.

2.6. Extraction and mass spectrometry of molar proteins

Molar proteins were extracted and separated by 2D electrophoresis, as described previously (Tynyakov et al., 2015a) with slight modifications. For isoelectric focusing, the Immobiline dry strip (11 cm, pH 3–10) was rehydrated and aligned on an isoelectric focusing tray. The molar protein extract was loaded adjacent to the anode, and voltage was applied for a total of 11.9 kV-h. Following isoelectric focusing, the gel strip was equilibrated in a buffer comprising 6 M urea, 0.375 M Tris-HCl, pH 8.8, 2% SDS, and 20% glycerol and incubated in 2% dithiothreitol for reduction, followed by 8% iodoacetamide for alkylation. Then, the strip was mounted on 15% SDS-PAGE with the Tris/glycine running buffer system, as described previously (Lucas, 2004). Spots suspected of belonging to the MARS protein family were visualized with Coomassie Blue staining; gel pieces were excised and prepared for mass spectrometry as follows. Proteins in the molar extracts were trypsin digested, purified and dissolved as described previously (Tynyakov et al., 2015a). Nanoliquid chromatography and mass spectrometry analysis was performed as described previously (Glazer et al., 2010) using a 75-µm internal diameter fused silica column, packed with C18 (NewObjective, Woburn, MA, USA) and connected to an Eksigent nano-LC system (Eksigent, Dublin, CA, USA). Mass spectra were acquired using an LTQ-Orbitrap XL (ThermoFisher Scientific, San Jose, CA, USA) and analyzed using the PEAKS Mass Spectrometry Software. Protein validation was performed by the Sequest and Mascot algorithms operated under Proteome Discoverer 2.0 (ThermoFisher Scientific) against the deduced protein sequences of the entire molt-related transcriptomic library.

2.7. Histological preparations

The mandible of an early pre-molt animal was decalcified in a histological decalcifying agent (Calci-Clear Rapid; National Diagnostics, Atlanta, GA) with paraformaldehyde (4%) as a fixation agent. Samples were then dehydrated and embedded in paraffin and sectioned as previously described (Ventura et al., 2009). Sections (5 µm) were stained with hematoxylin and eosin and observed under a light microscope.

2.8. dsRNA production and silencing efficiency experiment

Two representative MARS genes, *MARS3* and *MARS4*, were selected for loss-of-function experiments using RNAi. These MARS proteins genes were selected since the entire MARS family was targeted and these MARS proteins genes had higher similarity to the other MARS protein genes. To synthesize dsRNA, two PCR products were generated using a T7 promoter anchor (T7P) attached to one of the two primers used to amplify each product. The primers used for generating the template for *MARS3* and *MARS4* sense-strand RNA synthesis were: as the forward primer dsMARS3F+T7 and dsMARS4F+T7, respectively, and as the reverse primer dsMARS3R and dsMARS4R, respectively. For *MARS3* and *MARS4* anti-sense strand RNA synthesis, the forward primers were dsMARS3F and dsMARS4F, respectively, and the reverse primer were dsMARS3R+T7 and dsMARS4R+T7' respectively. All primer sequences are shown in Table S5. PCR amplicons were separated and visualized, followed by dsRNA preparation, hybridization, quantification and maintenance, as described previously (Sharabi et al., 2013). For the silencing efficiency experiment, inter-molt *C. quadricarinatus* males (10–15 g) that were induced to molt were used. Animals were separated to two groups, a control group injected with an exogenous dsRNA of dsGFP (n = 5) and a treatment group injected with a mix of dsRNA of *MARS3* and *MARS4* (n = 5) (termed the dsMARS treatment). The concentration of dsRNA was 2 µg/g dsMARS per g body weight (i.e., 1 µg/g body weight for each MARS gene); the dose was determined in preliminary experiments, which showed optimal survival at that concentration (data not shown). The injections of dsRNA began when the animals reached an MMI of 0.02 and were given daily over a period of five days. On the sixth day, the animals were dissected, and mRNA from the mandible-forming epithelium was extracted, as described above. Relative expression of MARS encoding genes in the mandible-forming epithelium of the two groups was evaluated using qPCR, and statistical analyses were performed as described above.

2.9. Phenotypic effects following RNAi

To test for phenotypic effects in mandible formation, loss-of-function experiments were conducted in parallel to molt induction. Fourteen inter-molt *C. quadricarinatus* males (5–10 g) were induced to molt and divided to two groups, a control group injected with dsGFP (n = 8), and a treatment group injected with dsMARS mix (n = 6). The experiment was conducted with a dsRNA concentration of 2 µg/g body weight (i.e., 1 µg/g body weight for each MARS gene) and with the following injection routine: every two days one injection was given until early pre-molt; thereafter, injections were given on a daily basis for one week, followed by injections every two days until ecdysis. Animals at two days post-molt were anesthetized, as described above, and the newly formed mandible was dissected. This experimental design was used since it permitted better survival (data not shown) compared to daily injections. Incisor tooth sharpness was measured as previously described (Popowics and Fortelius, 1997). In brief, for each one of the incisor teeth, the base was regarded as 1 and was used as the basis for normalizing different sized teeth, then; the radius

(r) of the fitting circle within the tip was calculated. The calculated radius was then transformed to a blade sharpness index calculated as $1-r$. All analyses of tooth sharpness were performed on the left mandible incisor using ImageJ (Abramoff et al., 2004). Within each incisor, sharpness of teeth number 2–5, as shown in Fig. 6, was measured, yielding a tooth sharpness parameter. Kruskal-Wallis rank sum test was performed followed by multiple pair-wise comparisons using the Wilcoxon rank sum test comparing the sharpness of teeth number 2–5 between the control and silenced groups. $P < 0.05$ was considered statistically significant.

2.10. SEM and EDXS

For Scanning Electron Microscopy (SEM), incisor teeth were; air dried, separated to single tooth, manually fractured and then gold-coated for 6 s. All samples were characterized by a JEOL JSM-7400f electron microscope at the Ilse Katz Institute for Nanoscale Science & Technology, Beer Sheva, Israel. Measurements of calcium and phosphate count were determined using an Energy Dispersive X-ray Spectroscopy detector (EDXS, KeveX; Thermo Scientific, Scotts Valley, CA), the acceleration voltage was set on 25 kV and the EDXS signal was accumulated over 50 s. The calcium and phosphorus counts represent the integrated signal of the elements along the acquisition time. Raman spectroscopy was performed as previously described (Bentov et al., 2012).

2.11. Phylogenetic analysis

To find homologous MARS proteins in other species, a multiple sequence alignment (MSA) of the found MARS proteins from *C. quadricarinatus* was created using the editor Jalview (Clamp et al., 2004) based on Clustal Omega with default parameters. Based on this alignment, an HMMER profile was created using the UGENE software (Okonechnikov et al., 2012), which was then used to perform an “hmmsearch” with the HMMER web server (Finn et al., 2011). In addition, homologous proteins were searched in the following five NGS libraries: A transcriptome library from the Pacific white shrimp *L. vannamei* composed of a wide array of developmental stages [published by Wei et al. (2014)], a transcrip-

tome library from the Chinese shrimp *F. chinensis* composed of several individuals at 15 days post larvae stage (Li, personal communication), a transcriptome library from the ridgetail prawn *E. carinicauda* composed of several adult individuals with a body length about 5 cm (Li, personal communication), our transcriptomic library from the giant freshwater prawn *Macrobrachium rosenbergii* composed of a wide array of tissues and developmental stages (Sharabi et al., 2015), and the only publicly available crustacean-genome of the common water flea *Daphnia pulex* available online via: <http://wfleabase.org/> and described by Gilbert et al. (2005). Finally, representative MARS proteins from different crustaceans and an outgroup from an insect were used to build a maximum likelihood tree using MEGA6 software (Tamura et al., 2013), with default parameters, coupled to a bootstrap test set on 10×10^3 repetitions.

3. Results

3.1. Characterization of the Pre-Molt incisor and molar

The processes occurring during the formation of the mandible in the pre-molt stage were followed by optical and SEM microscopy. The formation of new mandibular structures could be seen during this stage (Fig. 1a and d), and the newly forming incisor (Fig. 1b) and molar (Fig. 1e) were clearly visible at the higher magnification. The underlying forming epithelium could be seen underneath the newly forming molar and incisor. For both the incisor and the molar, it was found that the tips of the teeth were formed in the pre-molt stage (Fig. 1b and d). SEM images of the newly forming incisor (Fig. 1c) showed fibers oriented vertically to the surface consisting of chitin-protein complex which are probably originating from the pore canal system. SEM images of the newly forming molar (Fig. 1f) revealed mineral deposition over a chitinous-fiber scaffold (Fig. S1).

3.2. The MARS protein family

To study the molecular basis underlying the formation of the above-described vertical elements, candidate structural proteins

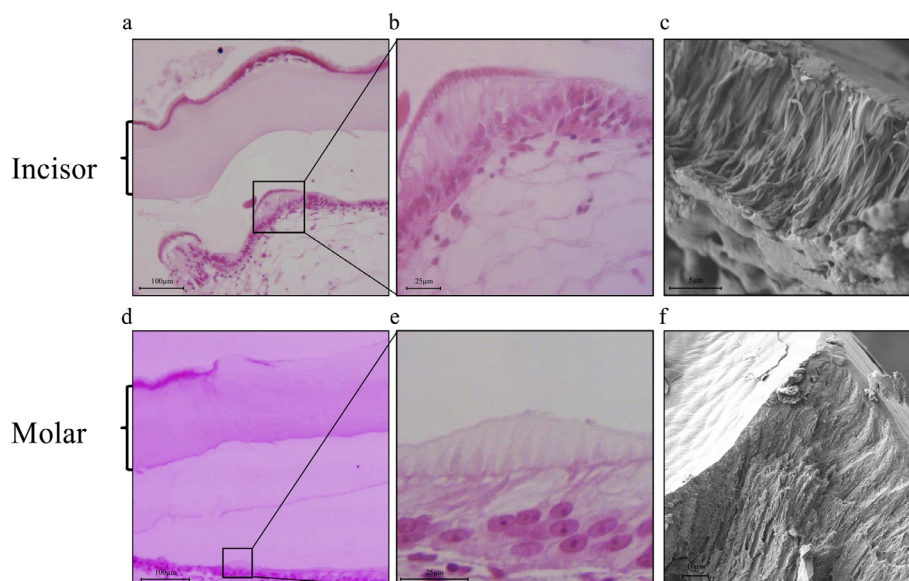


Fig. 1. Tips of the mandible teeth consisting of vertical elements that are formed during pre-molt. a) Optical micrographs of old (indicated with a brace) and newly formed incisor of a pre-molt animal and b) higher magnification of the newly formed incisor. c) SEM micrograph of the newly formed incisor. d) Optical micrographs of a pre-molt animal old (indicated with a brace) and newly formed molar and e) higher magnification of the newly formed molar. f) SEM micrograph of the newly formed molar. See also Fig. S1.

were mined from our mandible-forming epithelium molt-related transcriptomic libraries. A new gene family predicted to be involved in mandible formation was discovered and characterized. This newly revealed family, with almost 30% alanine in its deduced amino acid sequence (Table S1), was designated the Mandible Alanine Rich Structural (MARS) protein family. In total, four MARS protein family members were found in *C. quadricarinatus*: MARS1 (KY197784), MARS2 (AK187814), MARS3 (KY197785) and MARS4 (KY197786) (Fig. 2a). Sequence similarity among the four MARS proteins ranged from 49% to 66% (Table S2). Alanine was the most abundant amino acid, followed by glycine and glutamine (Table S1 and Fig. 2a). The predicted pI differed among the different family members, ranging from 5.8 to 9.1 (Table S3). A signal peptide was predicted in the N'-terminal of all the MARS proteins, followed by a predicted proprotein R(E/D)KR convertase cleavage site. Within the putative active protein, three modules were detected that are each enriched with particular amino acids in a repetitive manner. First is an N'-terminal glycine-rich module characterized by GGX repeats and conserved tyrosine residues (positions 37–76 in the alignment shown in Fig. 2a). This module is followed by a middle module rich in alanine and glutamine and characterized by AAX and AQ repeats (positions 77–243 in the alignment shown in Fig. 2a). The third module is a C'-terminal glycine-rich module

with sequential characteristics similar to those of the N'-terminal glycine-rich module (positions 244–265 in the alignment shown in Fig. 2a), as can be seen in Fig. 2. Secondary structure prediction using XtalPred showed that the MARS proteins are mostly intrinsically disordered, with regions predicted to be disordered also found in parallel to regions predicted to form a secondary structure, such as α -helices (Fig. S2).

3.3. Spatial and temporal expression

Spatial and temporal expression experiments were performed to elucidate the timing and location of MARS expression in the mandible-forming epithelium compared to other skeletal and somatic tissues. The four MARS genes were expressed at all the molt stages, mainly in the mandible-forming epithelium, including the molar- and incisor-forming epithelia. Only in the early pre-molt stage were these genes expressed in another skeletal element, the gastrolith-forming epithelium (Fig. 3).

3.4. Expression-pattern during the molt cycle

To further investigate the possible involvement of the MARS protein family in mandible formation, qPCR quantifying the

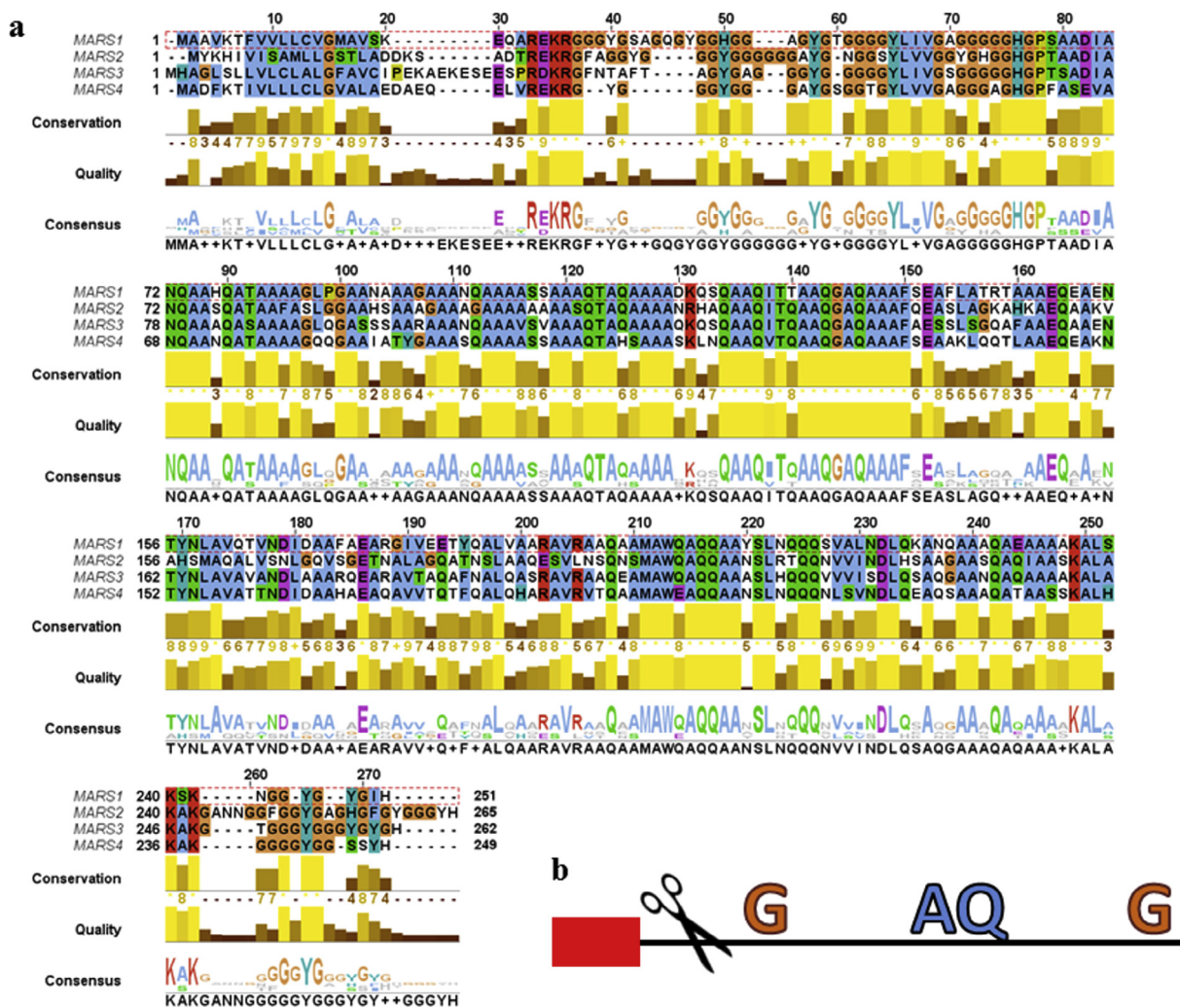


Fig. 2. Sequence characteristics of the putative MARS proteins, including a signal peptide, a conserved cleavage site, and glycine-, alanine- and glutamine-enriched regions. a) Multiple sequence alignment of the MARS proteins found in *C. quadricarinatus*. For each position in the sequence-alignment, the conservation, degree, alignment, quality, and consensus logo sequence are shown below. b) A schematic representation of the "general" MARS protein. Red box represents a signal peptide, scissors represent the R(E/D)KR cleavage site, which is followed by an N'-terminal glycine-enriched domain (G), an alanine-glutamine-enriched domain (AQ), and a C'-terminal glycine-enriched domain (G). See also Fig. S2 and Table S1–S3.

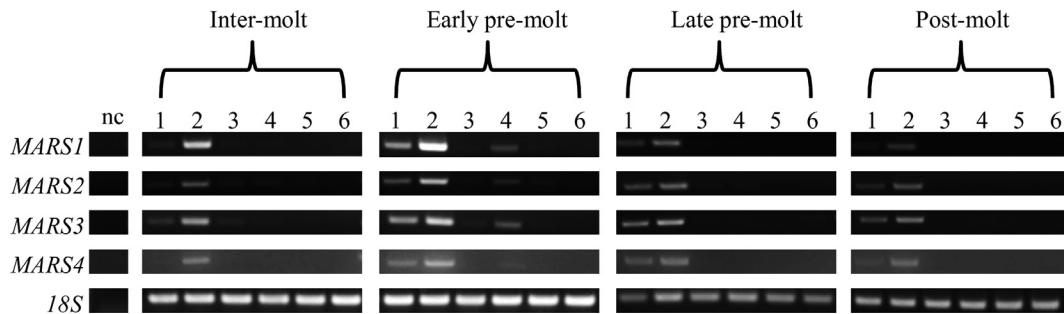


Fig. 3. Spatial-temporal expression of the MARS protein-encoding genes expressed mainly in mandibular-forming epithelium. For each gene, spatial-temporal expression is shown in the following six tissues sampled in animals at four different molt stages: 1 – molar-forming epithelium, 2 – incisor-forming epithelium, 3 – carapace cuticle-forming epithelium, 4 – gastrolith-forming epithelium, 5 – hepatopancreas, and 6 – abdominal muscle. nc – negative control.

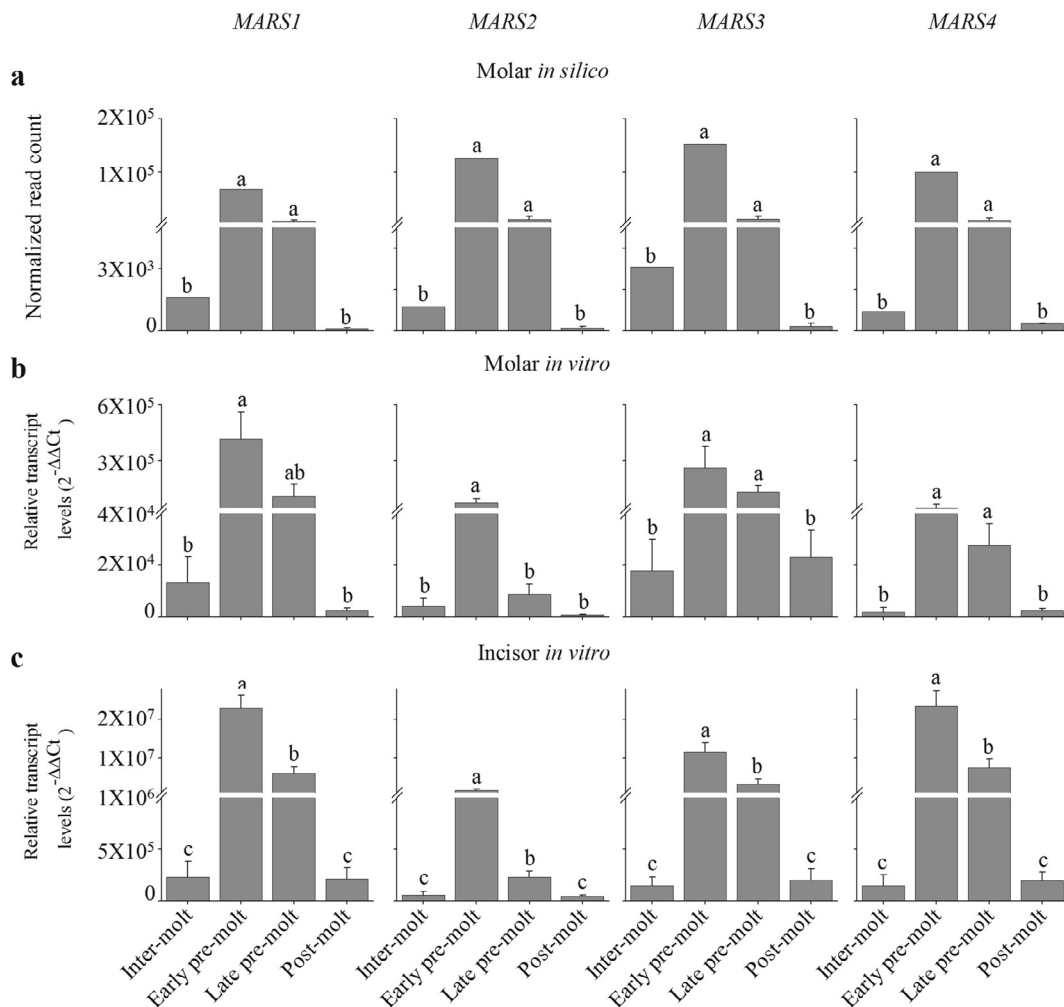


Fig. 4. In the mandibular-forming epithelium, the MARS genes are highly expressed at pre-molt. a) Read count of the MARS genes in the molt-related transcriptomic library originating from the molar-forming epithelium. b) Relative levels of the MARS genes in the molar-forming epithelium in four molt stages, as determined by qPCR. For all molt stages $n = 5$. c) Relative levels of the MARS genes in the incisor-forming epithelium in four molt stages, as determined by qPCR. For all molt stages, $n = 5$. The four molt stages, namely, inter-molt, early pre-molt, late pre-molt and post-molt, are represented on the X axis. For all sections, different letters represent groups that are significantly different ($p < 0.05$); error bars represent standard error.

expression during the molt cycle in the mandible-forming epithelium was performed. This method was used first to validate *in vitro* the pre-molt related expression pattern of MARS-protein-encoding genes in the molar-forming epithelium, as found *in silico* in the molt-related transcriptomic library (Fig. 4a). qPCR was also used to provide information on the MARS protein expression pattern in the incisor-forming epithelium. The pre-molt-related expression

pattern in the molar-forming epithelium was verified *in vitro* for all the MARS genes with the exception of MARS1 for which late pre-molt expression was not significantly different from post-molt expression (Fig. 4b). The pre-molt-related expression patterns were basically similar in the incisor- and molar-forming epithelia (Fig. 4c) but with a few differences: In the incisor-forming epithelium – but not in the molar-forming epithelium – expression in the

early pre-molt period was significantly higher than in the late pre-molt period. In addition, calculated relative quantification (RQ) levels during early pre-molt were $\approx 10^2$ higher in the incisor-forming epithelium than in the molar-forming epithelium (Fig. 4b and c).

3.5. Identification of a MARS protein in the mandible

The determination of MARS proteins in the mandible was performed by extracting the proteins, followed by separation by 2D electrophoresis and identification by mass spectrometry. The process resulted in the localization of only one MARS family protein in a prominent dot in the 2D gel (Fig. 5). The protein was identified as

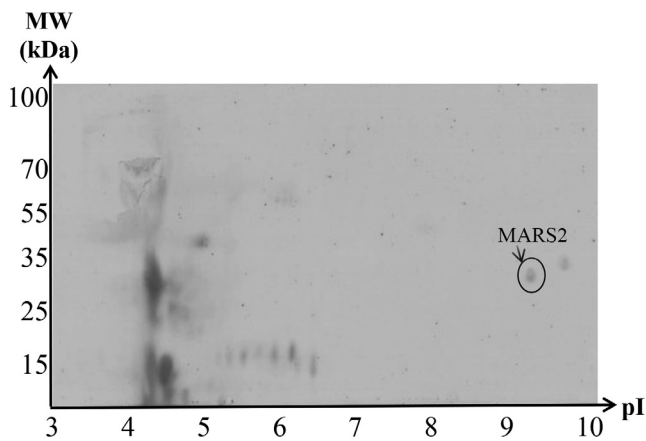


Fig. 5. Two-dimensional electrophoresis of *C. quadricarinatus* molar proteins. Related to Figs. 3 and 4. Proteins extracted from mandible cuticle were separated on a linear 3–10 pI gradient. Following mass spectrometry and peptide identification, a prominent MARS2 spot was identified (indicated with a circle) in the 27-kDa spot at pI ≈ 9.3 . See also Table S3.

MARS2 with a molecular mass of 27 kDa and a pI of ≈ 9.3 -values that were similar to the predicted size and pI of MARS2.

3.6. Silencing efficiency

In preparation for the loss-of-function experiment, the reduction in gene expression following injections with dsMARS mix MARS3 and 4 was evaluated using qPCR. The specific silencing showed a significant decrease in gene expression between the control (dsGFP injected) and treatment groups, with 90% efficiency for MARS3 and 99% efficiency for MARS4. In addition, another MARS encoding gene was significantly silenced when the dsMARS mix was injected, i.e. MARS1 which was silenced with 65% efficiency (Fig. S3).

3.7. Phenotypic effects of the loss-of-function experiments

To study the role of MARS proteins, RNAi-based loss-of-function experiments were conducted to study mandible formation. Clear phenotypic differences between the control and silenced groups in the shape and ultrastructure of the incisor teeth were detected. While in the control group the incisor teeth were sharp, with pointed serrations possessing a triangular form, in the silenced group the teeth exhibited semi-circular scallops with surface irregularities, as can be seen in the representative incisors depicted in Fig. 6a. The significant reduction in tooth sharpness in the silenced group vs the control group is clearly demonstrated in Fig. 6b.

To better understand the differences in tooth composition, electron microscopy was utilized. Imaging of a section of an incisor from the control group showed the typical arrangement of the different layers within the incisor tooth (Fig. 7a). The bottom layer ($\approx 120 \mu\text{m}$) arranged horizontally to the surface showed the typical plywood pattern of the crustacean cuticle. The middle layer ($\approx 200 \mu\text{m}$) oriented vertically to the surface was built up of tightly

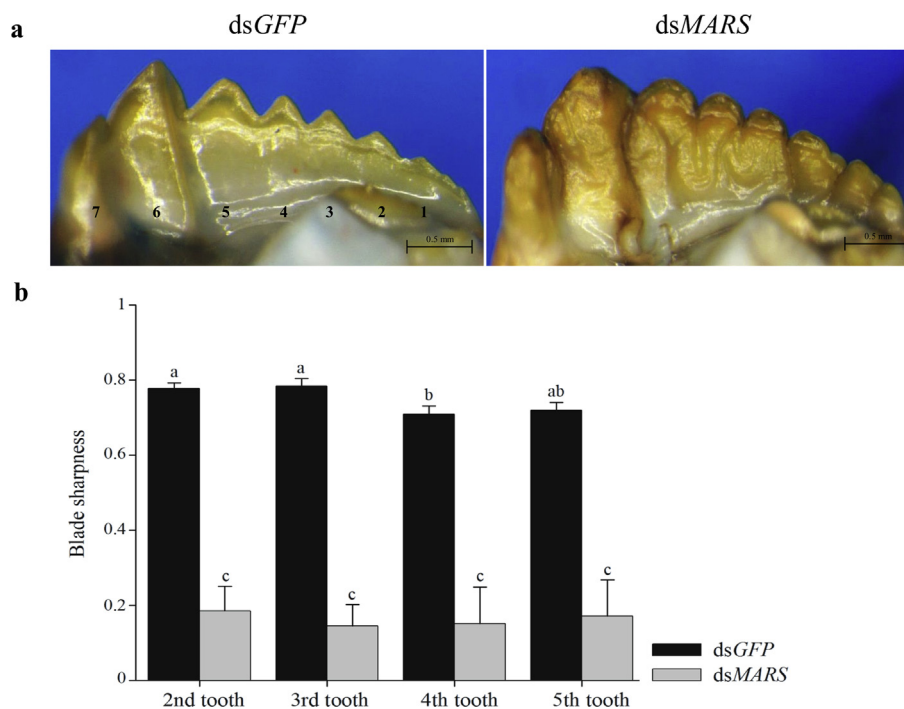


Fig. 6. Phenotypic effects following loss-of-function experiments in the incisor teeth of *C. quadricarinatus*. a) Representative left mandible incisors of animals from the dsGFP-injected control group (left) and dsMARS-injected group (right). Numbering of the incisor teeth is shown for the dsGFP-injected group. b) Blade sharpness results for tooth numbers 2–5 of the left mandible incisor of animals injected with dsGFP (n = 8) compared to animals injected with dsMARS (n = 6). Letters represent statistical groups that are significantly different ($p < 0.05$); error bars represent standard error. See also Figs. S4 and S5.

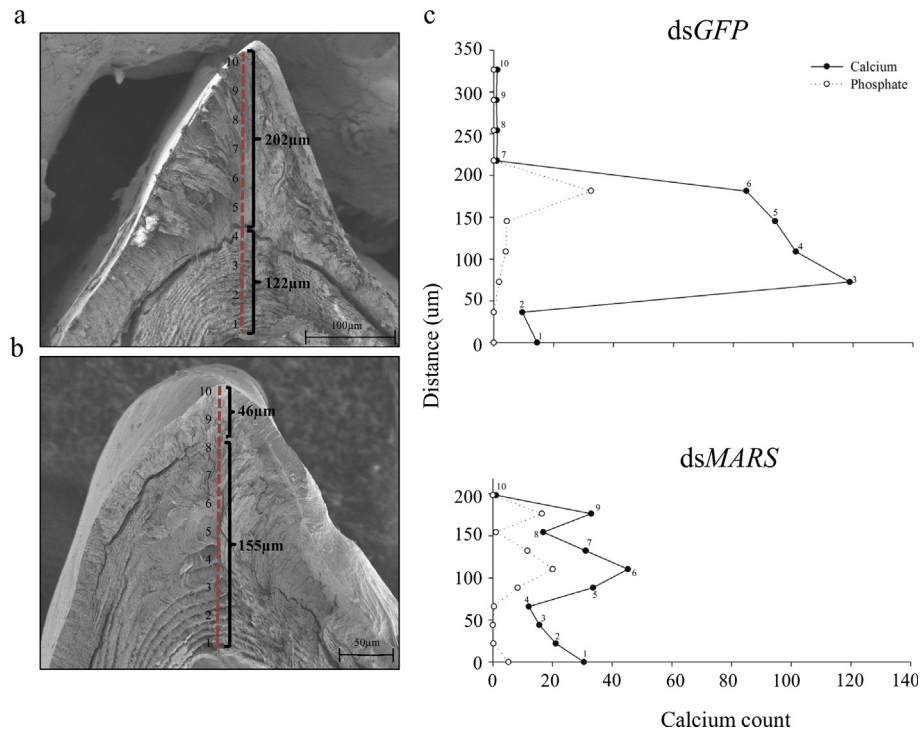


Fig. 7. Phenotypic effects following loss-of-function experiments on the formation of a horizontally arranged chitin layer in the incisor-teeth. a&b) SEM micrographs of a representative cross-section of an incisor tooth of an animal from the dsGFP-injected and dsMARS-injected groups, respectively. The two layers found in the incisor and their thickness is indicated. c) Calcium and phosphate count calculated using EDXS along the central axis of a cross section of an incisor tooth from the dsGFP-injected group (top) and the dsMARS-injected group (bottom). The dashed red line including the point's number in the electron micrographs shows the positions from which the EDXS results were taken. See also Figs. S4 and S5.

packed fibers and followed the typical triangular shape of the incisor tooth, showing a ratio of vertical layer thickness to horizontal layer thickness of 1.63. This layer was covered with an outer layer ($\approx 6 \mu\text{m}$) of non-fibrous matter (Fig. S4a). In the incisor from the silenced group, the bottom and top layers were similar to those of the control group with a bottom layer of ($\approx 155 \mu\text{m}$). The middle layer in the silenced group was of irregular orientation (Fig. S4b) and dramatically reduced to a thickness of $\approx 46 \mu\text{m}$ (Fig. 7b) showing a ratio of vertical layer thickness to horizontal layer thickness of 0.29. A similar outer layer of non-fibrous matter ($\approx 5 \mu\text{m}$) is seen in the silenced group (Fig. S6b). A qualitative calcium and phosphate count [energy-dispersive X-ray spectroscopy (EDXS) analysis] along the central axis of the incisor aiming to test for the presence or absence of these minerals in both the control and silenced teeth showed that the minerals were deposited in the inner part of the tooth starting along the bottom of the vertically oriented layer and continuing in the horizontally oriented layer, while no calcification was detected at the top of the vertically oriented middle layer (Fig. 7c).

Raman analyses of incisor teeth from the silenced and control groups showed no differences between the two groups in the composition of the different layers. The Raman peaks at $\sim 1104 \text{ cm}^{-1}$ have a major contribution from α -chitin vibrations (symmetric stretching of COC) and in experiments of chitin deproteinization, it is used to identify chitin vs. proteins (Iconomidou et al., 2001; Serrano et al., 2016). The peak at $\sim 1004 \text{ cm}^{-1}$ is a typical indicator of proteins (Phen), especially in crustacean cuticle in which sclerotization is exerted by phenolic cross linking. Thus, the peaks at $1104, 1004 \text{ cm}^{-1}$ can serve to estimate chitin/protein ratio and indeed the incisors fibers of the control and silenced group show both bands (various ratios), confirming that it is a chitin-protein complex. (Fig. S5a). The spectrum of the horizontal lower part showed peaks at 956 and 1085 cm^{-1} , indicating the presence of

amorphous calcium phosphate (ACP) and amorphous calcium carbonate (ACC), respectively, in addition to the presence of the carotenoid pigment astaxanthin, as indicated by prominent peaks at 1007 and 1157 cm^{-1} in both the treatment and control groups (Fig. S5b).

3.8. Phylogenetic analysis

Mining for homologous proteins was performed with the aim to study the evolutionary occurrence of MARS proteins in other crustaceans and pancrustaceans. Searching in available online databases revealed homologous proteins only in the branchiopod crustacean *Daphnia pulex* (13 proteins in total). In addition, a weak homology was found with several insect proteins; however, unlike the MARS proteins, the insect proteins also contained an unknown conserved domain (DUF745). Therefore, a representative DUF745-containing protein from an insect (the fly *Megaselia scalaris*) was used as an outgroup in our analysis. Searching for homologous proteins in the decapod crustaceans *Litopenaeus vannamei*, *Fenneropenaeus chinensis*, *Exopalaemon carinicauda* and *Macrobrachium rosenbergii* transcriptomic libraries (Sharabi et al., 2015) revealed several highly conserved MARS proteins. A phylogenetic tree constructed on the basis of representative MARS proteins from *C. quadricarinatus*, *L. vannamei*, *F. chinensis*, *E. carinicauda*, *Macrobrachium rosenbergii* and *Daphnia pulex* (Fig. 8) showed the presence of paralogous genes, such as in *Daphnia pulex*, in which the MARS proteins were found to be clustered together. Orthologous genes were found in *C. quadricarinatus*, *L. vannamei*, *F. chinensis*, *E. carinicauda* and *Macrobrachium rosenbergii*; for example, MARS3 proteins were clustered together, as seen in Fig. 8. Accession numbers of the different MARS proteins and the outgroup protein are given in Table S4.

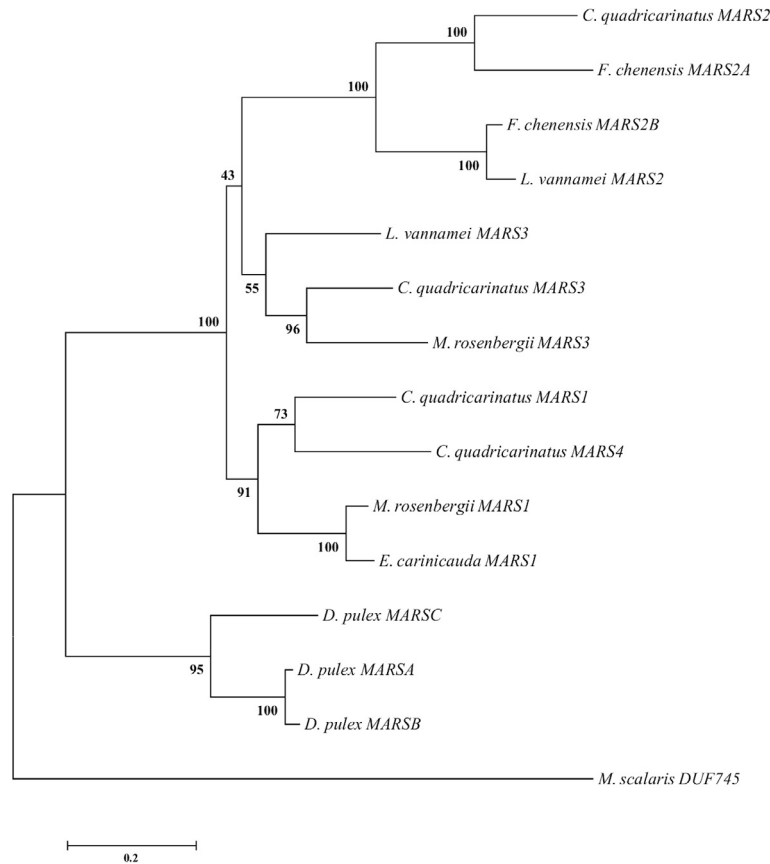


Fig. 8. Paralogues and orthologues of the MARS proteins found in different crustaceans. A maximum likelihood tree composed of MARS proteins from *C. quadricarinatus*, *L. vannamei*, *F. chinensis*, *E. carinicauda*, *Macrobrachium rosenbergii* and *D. pulex*. A non-crustacean protein from the fly *Megaselia scalaris* having an unknown domain (DUF745) and found to have similarity to the MARS proteins was used as an outgroup. Bootstrap test ($n = 1000$) results are shown at each node junction. See also Table S4.

4. Discussion

It has been suggested that the origin of organizations vertical to the surface of the crustacean skeleton lie in the pore canal system (Compere and Goffinet, 1987). Previous observations have focused on the co-occurrence of such vertical elements along with the horizontal organization comprising the greater part of the crustacean cuticle (Al-Sawalmih et al., 2008; Compere and Goffinet, 1987). Our recent study of vertical elements in the structure of the *C. quadricarinatus* molar showed that such elements occur towards the surface of the tooth without any horizontal organization (Bentov et al., 2012). In that study, we posited that this structural solution is related to the role of the molar in food processing [similarly to that suggested for the incisor of the isopod *P. scaber* (Bentov et al., 2012; Huber et al., 2014)], but we did not investigate such an organization in other mandibular locations, such as the incisor. The present study shows that in the *C. quadricarinatus* incisor, too, there is the typical vertical arrangement consisting of tightly packed chitin fibers oriented vertically to the surface. The function of such vertical elements in the incisor is probably also related to their role in food processing by providing reinforcement in the load-bearing direction. Such an arrangement, which differs in orientation from the bulk of the horizontally layered crustacean cuticle, seems to be a specialized cuticular structure that has evolved in crustaceans.

An important question arising from the above-described observations is: From which cuticular layer does the chitinous vertical arrangement originate? Such a question has been asked previously with regard to the layer of non-mineralized vertical elements in the incisor tip in *P. scaber* (Huber et al., 2014). At that time, with no knowledge regarding the timing of formation and type of mate-

rial of these vertical elements, it would have been difficult to give a definitive answer. In the present study, the timing of the formation of the vertically oriented chitin fibers in the mandible was found to be the pre-molt stage, i.e., concomitant with the formation of the epicuticle and exocuticle layers, indicating that the vertical chitin layer could be derived from either one of these two layers. The presence of phenolic compounds indicates sclerotization processes (Andersen, 2010; Hasson and Sugumaran, 1987), which are typical of the epicuticle (Cloudsley-Thompson, 1950), including its vertical elements (Vatcher et al., 2015). However, the logical choice is the exocuticle, a thick layer comprising tightly packed chitin fibers (Roer and Dillaman, 1984), rather than the epicuticle, the outermost skeletal layer, which is known to be a thin non-chitinous layer. Therefore, we assume that the vertically oriented chitin fibers in *C. quadricarinatus* mandibles are specialized elements of exocuticular origin. We posit that the horizontally arranged chitin fibers have vanished from this specialized exocuticle and that the pore canal system dominates the structure, suggesting a clear evolutionary advantage.

The similarities between the incisor and the molar teeth of *C. quadricarinatus* in terms of timing of formation, structure and, presumably, a common origin suggests common biochemical mechanisms and gene regulation. Therefore, we suggest that specialized mandible-forming proteins, in particular, the novel MARS proteins discovered in this study, are part of such a specialized toolkit for structural assembly. The predicted MARS proteins have a modular sequence design in which each module is characterized by enrichment in specific amino acids with the alanine/glutamine-rich module spanning most of the sequence of the MARS proteins. Alanine has a high helix propensity (Chakrabarty et al., 1994), with

glutamine stabilizing the helical structures (Vila et al., 2000), which indicates a possible helical structure for the MARS proteins. The presence of predicted intrinsically disordered regions (IDRs) in parallel to the predicted α -helices suggests that the MARS protein secondary structure might be formed only upon binding to a substrate, as found for other IDR-bearing proteins exhibiting a disorder-to-order transition (Dyson and Wright, 2002; Vuzman and Levy, 2012). Such a substrate in the extracellular matrix is likely to be another structural protein, possibly another MARS protein, with two different MARS proteins interacting to create a supercoil structure. Other known invertebrate structural proteins having a similar modular design are the suckerin proteins, which are involved in the formation of the squid sucker teeth (Ding et al., 2014) and in many known spider silk protein sequences (Gatesy et al., 2001; Hayashi et al., 1999). The latter proteins form fibers through inter- and intra-molecular interactions. This type of design is therefore known in fiber-forming structural proteins involved in the formation of stiff biological materials, suggesting that the MARS proteins might act as fiber-forming structural proteins enhancing the stiffness of the extracellular matrix.

The results of the investigation of temporal and spatial expression of MARS proteins suggest a specialized role for these proteins in mandible formation. Timing of the expression of the MARS encoding genes during the molt cycle shows a clear relation of protein expression to pre-molt during which the mandible vertical elements are formed. Such a pattern was also found in a protein involved in molar mineralization (Tynyakov et al., 2015b). The putative role of the MARS proteins in mandible formation is also suggested by the presence of MARS family proteins in the mature mandibles. The fact that only MARS2 was found in our experiments to extract and separate mandibular proteins on a 2D gel might be due to technical difficulties obtaining a sufficient amount of detectable protein from the small-sized cuticular mandibular elements.

Loss-of-function experiments using RNAi have been used previously to provide a clear phenotypic indication of the roles of matrix proteins (Glazer et al., 2010; Shechter et al., 2008b). In the current study, the central role of MARS proteins was exemplified by alterations in the phenotypic ultrastructure of the incisor tooth, in which the vertically oriented layer almost completely collapsed showing an irregular arrangement in response to silencing. EDXS results confirmed this observation, showing a net reduction in the thickness of the non-calcified layer composed of the vertically oriented chitinous elements. The irregular phenotype showing a reduction in tooth sharpness, which would affect the efficiency of the incisor as a food processing apparatus, suggests that MARS proteins are crucial for survival.

It was hypothesized many years ago that specialized proteins play a role in the formation of vertical chitinous elements (Comper and Goffinet, 1987). The exact role of the MARS proteins in the formation of such elements is as yet unclear, but a hint can be found in the silencing experiment results, namely, in our findings that no structural abnormalities were seen in calcified vertical elements in the molar, which are heavily calcified already at pre-molt (Tynyakov et al., 2015a), as opposed to the lack of calcification in the vertical chitinous elements of the incisor. It is noteworthy that calcification assists in the reinforcement of mineralized horizontally layered cuticles (Huber et al., 2015) and even more so for vertical elements that need additional support. Thus, MARS proteins seem to be involved in reinforcement along the normal axis of vertically oriented chitin fibers, which explains the structural collapse in the absence of MARS proteins.

It is logical that the involvement of MARS proteins in the vertical arrangement of chitin fibers would include a linkage between the proteins and the chitinous scaffold. In the absence of a chitin-binding domain in the MARS proteins, a possible linkage

mechanism would be crosslinking of the proteins to other chitin-binding proteins or directly to the chitinous scaffold through sclerotization, as is known in arthropods (Andersen, 2010; Roer et al., 2015). The highly conserved lysine residues in the C'-terminal of the MARS proteins might take part in such a linkage, since these residues are involved in crosslinking in the process of sclerotization (Andersen and Roepstorff, 2007; Gordon and Carriker, 1980). The modular design of the MARS proteins, which are presumed to form fibrils (Guerette et al., 1996, 2014; Hayashi et al., 1999), might provide the orientation of the structure such that the predicted reinforcement of the vertical chitinous elements is towards the normal axis.

MARS protein homologs were found by us in a wide array of crustacean libraries, from *Daphnia* to decapods, including several cases of orthologous and paralogous proteins. This conservation is probably due to a strong evolutionary pressure based on the importance of the vertically reinforced specialized mandibular-structure for food capture and processing. Proteins having a weak homology to the MARS protein family, found in numerous prominent insects such as *Drosophila melanogaster*, *Tribolium castaneum* and *Megaselia scalaris*, indicate a possible pancrustacean ancestor protein. Unlike the MARS proteins found in the present study, the insect homologs all contain a DUF745 domain, implying that they might belong to an as-yet uncharacterized insect protein family. To the best of our knowledge, no studies have been conducted on DUF745-containing proteins in insects, meaning that their role is still unknown.

In conclusion, the structural complexity of the mandible of *C. quadricarinatus* answers the need for a variety of tooth functionalities. The biochemical mechanisms that have evolved concomitant to the formation of such structural complexity include the novel MARS structural protein family. It appears that this protein family specializes in the support of vertical chitin fibers in the mandible teeth, providing structural reinforcement and maintaining the teeth in the correct orientation. The molecular function of the MARS proteins is predicted to be linked to their modular sequence design. Similar sequences have been suggested in the past to support fiber formation (Ding et al., 2014; Guerette et al., 2014; Hayashi et al., 1999). The results of the current study therefore provide the first valuable insights into the evolution and molecular mechanism underlying the formation of vertical organizations in high-impact regions of the crustacean skeleton.

Acknowledgements

This study was supported in part by grants from the Israel Science Foundation (ISF, Grant 102/09), the Israel Science Foundation – Israel and the National Natural Science Foundation of China – China (ISF-NSFC Grant 613/13) and the National Institute for Biotechnology in the Negev (NIBN). We would like to thank Dr. Roxana Golan from the Ilse Katz Institute for Nanoscale Science and Technology, Ben-Gurion University of the Negev for her valuable help with the SEM imaging.

Appendix A. Supplementary data

Supplementary data associated with this article can be found, in the online version, at <http://dx.doi.org/10.1016/j.jsb.2017.04.003>.

References

- Abehsera, S., Glazer, L., Tynyakov, J., Plaschkes, I., Chalifa-Caspi, V., Khalaila, I., Aflalo, E.D., Sagi, A., 2015. Binary gene expression patterning of the molt cycle: the case of chitin metabolism. *PLoS One* 10, e0122602.
- Abramoff, M.D., Magalhães, P.J., Ram, S.J., 2004. Image processing with ImageJ. *Biophotonics Int.* 11, 36–42.

- Al-Sawalmih, A., Li, C.H., Siegel, S., Fabritius, H., Yi, S.B., Raabe, D., Fratzl, P., Paris, O., 2008. Microtexture and chitin/calcite orientation relationship in the mineralized exoskeleton of the American lobster. *Adv. Funct. Mater.* 18, 3307–3314.
- Altschul, S.F., Gish, W., Miller, W., Myers, E.W., Lipman, D.J., 1990. Basic local alignment search tool. *J. Mol. Biol.* 215, 403–410.
- Andersen, S.O., 2010. Insect cuticular sclerotization: a review. *Insect Biochem. Mol. Biol.* 40, 166–178.
- Andersen, S.O., Roepstorff, P., 2007. Aspects of cuticular sclerotization in the locust, *Scistocerca gregaria*, and the beetle, *Tenebrio molitor*. *Insect Biochem. Mol. Biol.* 37, 223–234.
- Bentov, S., Zaslansky, P., Al-Sawalmih, A., Masic, A., Fratzl, P., Sagi, A., Berman, A., Aichmayer, B., 2012. Enamel-like apatite crown covering amorphous mineral in a crayfish mandible. *Nat. Commun.* 3, 839.
- Chakrabarty, A., Kortemme, T., Baldwin, R.L., 1994. Helix propensities of the amino acids measured in alanine-based peptides without helix-stabilizing side-chain interactions. *Protein Sci.* 3, 843–852.
- Chateigner, D., Hedegaard, C., Wenk, H.R., 2000. Mollusc shell microstructures and crystallographic textures. *J. Struct. Geol.* 22, 1723–1735.
- Clamp, M., Cuff, J., Searle, S.M., Barton, G.J., 2004. The Jalview Java alignment editor. *Bioinformatics* 20, 426–427.
- Cloudsley-Thompson, J.L., 1950. Epicuticle of arthropods. *Nature* 165, 692–693.
- Compere, P., Goffinet, G., 1987. Ultrastructural shape and three-dimensional organization of the intracuticular canal systems in the mineralized cuticle of the green crab *Carcinus maenas*. *Tissue Cell* 19, 839–857.
- DiMasi, E., Sarikaya, M., 2004. Synchrotron X-ray microbeam diffraction from abalone shell. *J. Mater. Res.* 19, 1471–1476.
- Ding, D., Guerette, P.A., Hoon, S., Kong, K.W., Cornvik, T., Nilsson, M., Kumar, A., Lescar, J., Miserez, A., 2014. Biomimetic production of silk-like recombinant squid sucker ring teeth proteins. *Biomacromolecules* 15, 3278–3289.
- Dosztanyi, Z., Csizmok, V., Tompa, P., Simon, I., 2005. IUPred: web server for the prediction of intrinsically unstructured regions of proteins based on estimated energy content. *Bioinformatics* 21, 3433–3434.
- Duckert, P., Brunak, S., Blom, N., 2004. Prediction of proprotein convertase cleavage sites. *Protein Eng. Des. Sel.* 17, 107–112.
- Dyson, H.J., Wright, P.E., 2002. Coupling of folding and binding for unstructured proteins. *Curr. Opin. Struct. Biol.* 12, 54–60.
- Finn, R.D., Clements, J., Eddy, S.R., 2011. HMMER web server: interactive sequence similarity searching. *Nucleic Acids Res.* 39, W29–37.
- Gasteiger, E., Hoogland, C., Gattiker, A., Duvaud, S.E., Wilkins, M.R., Appel, R.D., Bairoch, A., 2005. Protein Identification and Analysis Tools on the ExPASy Server. Springer.
- Gatesy, J., Hayashi, C., Motriuk, D., Woods, J., Lewis, R., 2001. Extreme diversity, conservation, and convergence of spider silk fibroin sequences. *Science* 291, 2603–2605.
- George, R.A., Heringa, J., 2000. The REPRO server: finding protein internal sequence repeats through the Web. *Trends Biochem. Sci.* 25, 515–517.
- Gilbert, D., Singan, V., Colbourne, J., 2005. WfleaBase: the *Daphnia* genomics information system. *BMC Bioinformatics* 6, 45.
- Glazer, L., Shechter, A., Tom, M., Yudkovski, Y., Weil, S., Aflalo, E.D., Pamuru, R.R., Khalaila, I., Bentov, S., Berman, A., Sagi, A., 2010. A protein involved in the assembly of an extracellular calcium storage matrix. *J. Biol. Chem.* 285, 12831–12839.
- Gordon, J., Carriker, M., 1980. Sclerotized protein in the shell matrix of a bivalve mollusc. *Mar. Biol.* 57, 251–260.
- Guerette, P.A., Ginzinger, D.G., Weber, B.H., Gosline, J.M., 1996. Silk properties determined by gland-specific expression of a spider fibroin gene family. *Science* 272, 112–115.
- Guerette, P.A., Hoon, S., Ding, D., Amini, S., Masic, A., Ravi, V., Venkatesh, B., Weaver, J.C., Miserez, A., 2014. Nanoconfined beta-sheets mechanically reinforce the supra-biomolecular network of robust squid Sucker Ring Teeth. *ACS Nano* 8, 7170–7179.
- Hasson, C., Sugumaran, M., 1987. Protein cross-linking by peroxidase: possible mechanism for sclerotization of insect cuticle. *Arch. Insect Biochem. Physiol.* 5, 13–28.
- Hayashi, C.Y., Shipley, N.H., Lewis, R.V., 1999. Hypotheses that correlate the sequence, structure, and mechanical properties of spider silk proteins. *Int. J. Biol. Macromol.* 24, 271–275.
- Huber, J., Fabritius, H.O., Griesshaber, E., Ziegler, A., 2014. Function-related adaptations of ultrastructure, mineral phase distribution and mechanical properties in the incisive cuticle of mandibles of *Porcellio scaber* Latreille, 1804. *J. Struct. Biol.* 188, 1–15.
- Huber, J., Griesshaber, E., Nindiyasari, F., Schmahl, W.W., Ziegler, A., 2015. Functionalization of biomineral reinforcement in crustacean cuticle: calcite orientation in the partes incisivae of the mandibles of *Porcellio scaber* and the supralittoral species *Tylos europaeus* (Oniscidea, Isopoda). *J. Struct. Biol.* 190, 173–191.
- Iconomidou, V.A., Chryssikos, G.D., Gionis, V., Willis, J.H., Hamodrakas, S.J., 2001. “Soft”-cuticle protein secondary structure as revealed by FT-Raman, ATR FT-IR and CD spectroscopy. *Insect Biochem. Mol. Biol.* 31, 877–885.
- Lucas, P.W., 2004. Dental Functional Morphology: How Teeth Work. Cambridge University Press.
- Miller, C.B., Nelson, D.M., Weiss, C., Soeldner, A.H., 1990. Morphogenesis of opal teeth in calanoid copepods. *Mar. Biol.* 106, 91–101.
- Nesbit, K.T., Roer, R.D., 2016. Silicification of the medial tooth in the blue crab *Callinectes sapidus*. *J. Morphol.* 277, 1648–1660.
- Okonechnikov, K., Golosova, O., Fursov, M., Team, U., 2012. Unipro UGENE: a unified bioinformatics toolkit. *Bioinformatics* 28, 1166–1167.
- Petersen, T.N., Brunak, S., von Heijne, G., Nielsen, H., 2011. SignalP 4.0: discriminating signal peptides from transmembrane regions. *Nat. Methods* 8, 785–786.
- Popowicz, T.E., Fortelius, M., 1997. On the cutting edge: tooth blade sharpness in herbivorous and faunivorous mammals. *Ann. Zool. Fenn.*, 73–88 JSTOR.
- Roer, R., Dillaman, R., 1984. The structure and calcification of the crustacean cuticle. *Am. Zool.* 24, 893–909.
- Roer, R., Abehsera, S., Sagi, A., 2015. Exoskeletons across the pancrustacea: comparative morphology, physiology, biochemistry and genetics. *Integr. Comp. Biol.* 55, 771–791.
- Serrano, C.V., Leemreize, H., Bar-On, B., Barth, F.G., Fratzl, P., Zolotoyabko, E., Politi, Y., 2016. Ordering of protein and water molecules at their interfaces with chitin nano-crystals. *J. Struct. Biol.* 193, 124–131.
- Sharabi, O., Ventura, T., Manor, R., Aflalo, E.D., Sagi, A., 2013. Epidermal growth factor receptor in the prawn *Macrobrachium rosenbergii*: function and putative signaling cascade. *Endocrinology* 154, 3188–3196.
- Sharabi, O., Manor, R., Weil, S., Aflalo, E.D., Lezer, Y., Levy, T., Aizen, J., Ventura, T., Mather, P.B., Khalaila, I., Sagi, A., 2015. Identification and characterization of an insulin-like receptor involved in crustacean reproduction. *Endocrinology*. en20151391.
- Shechter, A., Berman, A., Singer, A., Freiman, A., Grinstein, M., Erez, J., Aflalo, E.D., Sagi, A., 2008a. Reciprocal changes in calcification of the gastrolith and cuticle during the molt cycle of the red claw crayfish *Cherax quadricarinatus*. *Biol. Bull.* 214, 122–134.
- Shechter, A., Glazer, L., Cheled, S., Mor, E., Weil, S., Berman, A., Bentov, S., Aflalo, E.D., Khalaila, I., Sagi, A., 2008b. A gastrolith protein serving a dual role in the formation of an amorphous mineral containing extracellular matrix. *Proc. Natl. Acad. Sci. U.S.A.* 105, 7129–7134.
- Sievers, F., Higgins, D.G., 2014. Clustal Omega, accurate alignment of very large numbers of sequences. In: *Multiple Sequence Alignment Methods*. Springer, pp. 105–116.
- Slabinski, L., Jaroszewski, L., Rychlewski, L., Wilson, I.A., Lesley, S.A., Godzik, A., 2007. XtalPred: a web server for prediction of protein crystallizability. *Bioinformatics* 23, 3403–3405.
- Tamano, K., Stecher, G., Peterson, D., Filipiski, A., Kumar, S., 2013. MEGA6: molecular evolutionary genetics analysis version 6.0. *Mol. Biol. Evol.* 30, 2725–2729.
- Tynyakov, J., Bentov, S., Abehsera, S., Khalaila, I., Manor, R., Katzir, A.L., Weil, S., Aflalo, E., Sagi, A., 2015a. A novel chitin binding crayfish molar tooth protein with elasticity properties. *PLoS One* 10, e0127871–e0127871.
- Tynyakov, J., Bentov, S., Abehsera, S., Yehezkel, G., Roth, Z., Khalaila, I., Weil, S., Berman, A., Plaschkes, I., Tom, M., Aflalo, E.D., Sagi, A., 2015b. A crayfish molar tooth protein with putative mineralized exoskeletal chitinous matrix properties. *J. Exp. Biol.* 218, 3487–3498.
- Vatcher, H.E., Roer, R.D., Dillaman, R.M., 2015. Structure, molting, and mineralization of the dorsal ossicle complex in the gastric mill of the blue crab, *Callinectes sapidus*. *J. Morphol.* 276, 1358–1367.
- Ventura, T., Manor, R., Aflalo, E.D., Weil, S., Raviv, S., Glazer, L., Sagi, A., 2009. Temporal silencing of an androgenic gland-specific insulin-like gene affecting phenotypical gender differences and spermatogenesis. *Endocrinology* 150, 1278–1286.
- Vila, J.A., Ripoll, D.R., Scheraga, H.A., 2000. Physical reasons for the unusual alpha-helix stabilization afforded by charged or neutral polar residues in alanine-rich peptides. *Proc. Natl. Acad. Sci. U.S.A.* 97, 13075–13079.
- Vuzman, D., Levy, Y., 2012. Intrinsically disordered regions as affinity tuners in protein-DNA interactions. *Mol. Biosyst.* 8, 47–57.
- Wei, J., Zhang, X., Yu, Y., Huang, H., Li, F., Xiang, J., 2014. Comparative transcriptomic characterization of the early development in pacific white shrimp *Litopenaeus vannamei*. *PLoS One* 9, e106201.
- Weiner, S., Dove, P.M., 2003. An overview of biomineralization processes and the problem of the vital effect. *Rev. Mineral Geochem.* 54, 1–29.